Journal of Materials Science & Technology 34 (2018) 1061–1066

Contents lists available at ScienceDirect

Journal of Materials Science & Technology

journal homepage: www.jmst.org

Insight from *in situ* microscopy into which precipitate morphology can enable high strength in magnesium alloys

Bo-Yu Liu[a,1], Nan Yang[a,1], Jian Wang[b], Matthew Barnett[c], Yun-Chang Xin[d], Di Wu[e], Ren-Long Xin[d], Bin Li[f], R. Lakshmi Narayan[a,g], Jian-Feng Nie[h], Ju Li[a,i], Evan Ma[a,j,*], Zhi-Wei Shan[a,*]

[a] *Center for Advancing Materials Performance from the Nanoscale (CAMP-Nano) & Hysitron Applied Research Center in China (HARCC), State Key Laboratory for Mechanical Behavior of Materials, Xi'an Jiaotong University, Xi'an 710049, People's Republic of China*
[b] *Mechanical and Materials Engineering, University of Nebraska-Lincoln, Lincoln, NE 68588, USA*
[c] *Institute for Frontier Materials, Deakin University, Geelong, Victoria 3216, Australia*
[d] *College of Materials Science and Engineering, Chongqing University, Chongqing 400045, People's Republic of China*
[e] *Institute of Metal Research, Chinese Academy of Sciences, Shenyang 110016, People's Republic of China*
[f] *Department of Chemical and Materials Engineering, University of Nevada, Reno, USA*
[g] *Department of Materials Science and Engineering, Carnegie Mellon University, Pittsburgh, PA 15213, USA*
[h] *Department of Materials Science and Engineering, Monash University, Melbourne, Victoria 3800, Australia*
[i] *Department of Nuclear Science and Engineering and Department of Materials Science and Engineering, Massachusetts Institute of Technology, 77 Massachusetts Avenue, Cambridge, MA 02139, USA*
[j] *Department of Materials Science and Engineering, Johns Hopkins University, Baltimore, MD 21218, USA*

ARTICLE INFO

Article history:
Received 2 January 2018
Received in revised form 12 January 2018
Accepted 18 January 2018
Available online 14 February 2018

Keywords:
Precipitate selection criterion
In-situ TEM
Mg alloy
Mechanical property
Deformation twinning

ABSTRACT

Magnesium alloys, while boasting light weight, suffer from a major drawback in their relatively low strength. Identifying the microstructural features that are most effective in strengthening is therefore a pressing challenge. Deformation twinning often mediates plastic yielding in magnesium alloys. Unfortunately, due to the complexity involved in the twinning mechanism and twin-precipitate interactions, the optimal precipitate morphology that can best impede twinning has yet to be singled out. Based on the understanding of twinning mechanism in magnesium alloys, here we propose that the lamellar precipitates or the network of plate-shaped precipitates are most effective in suppressing deformation twinning. This has been verified through quantitative *in situ* tests inside a transmission electron microscope on a series of magnesium alloys containing precipitates with different morphology. The insight gained is expected to have general implications for strengthening strategies and alloy design.

1. Introduction

Lightweight magnesium (Mg) alloys are being actively pursued for their energy saving potential in fuel intensive transport [1,2]. However, the low strength of Mg alloys seriously hampers their broad applications. The idea of age hardening, inspired by success with Al alloys [3], has been widely applied to Mg alloys by introducing precipitates to enhance the strength. However, the strengthening effect is unsatisfactory [4] (Fig. S1). Different from Al alloys whose plasticity is governed exclusively by dislocation slips, yielding of Mg is usually subsidized by both dislocation slips on basal plane and deformation twinning (DT) on $\{10\bar{1}2\}$ plane (Fig. S2) [5]. The suppression of both basal slip and $\{10\bar{1}2\}$ DT is necessary in strengthening Mg alloys. For basal slips, the resistance from precipitates can be well quantified by Orowan model [6–8] and the strengthening effect is reliable [8–13]. However, from the experimental point of view, a consensus has yet to be reached whether the $\{10\bar{1}2\}$ DT can be effectively suppressed by precipitates [9–15] (Table S1). Although a few microscopy studies suggested that twin

* Corresponding authors at: Center for Advancing Materials Performance from the Nanoscale (CAMP-Nano) & Hysitron Applied Research Center in China (HARCC), State Key Laboratory for Mechanical Behavior of Materials, Xi'an Jiaotong University, Xi'an 710049, People's Republic of China.
E-mail addresses: ema.mse.jhu@gmail.com (E. Ma), zwshan@xjtu.edu.cn (Z.-W. Shan).
[1] These authors contributed equally to this work.

https://doi.org/10.1016/j.jmst.2018.01.017
1005-0302/

can be arrested by precipitates [16–19], they could not tell if twin can move again to pass through those precipitates, and how much stress increase would be needed for that to occur. The theoretically predicted best precipitates for blocking DT are prismatic plates [4,20], but DT can not be reduced by such precipitates in some experiments [10,14]. With readily activated $\{10\bar{1}2\}$ DT, Mg alloys still suffer from low strength [21]. Therefore, an effective precipitate morphology that can impede $\{10\bar{1}2\}$ DT to a great degree is pressingly needed for developing high strength Mg alloys.

The present work was inspired by an atomistic understanding of twinning mechanism in Mg. $\{10\bar{1}2\}$ DT can grow through the migration of basal-prismatic interfaces (BP) [22–25] and the twin is then not restricted on the $\{10\bar{1}2\}$ plane [26–28]. This facilitates the growth of $\{10\bar{1}2\}$ twin in a flexible manner (with liquid-like characteristics): when a part of the twin is pinned by precipitates, the other parts can still migrate via BP migration. A hint of this phenomenon is that the twin boundary is always curved when it intersects with precipitates [7,16–19,29,30]. As such, we hypothesize that if the precipitate entails a high aspect ratio (like a wall), or the precipitates connect with each other to form a three-dimensional network, the expanding twin would have a hard time bypassing or engulfing such an obstacle. When twinning becomes difficult, non-basal dislocation slips that originally do not come into play would necessarily become activated (Fig. S3). Fig. 1 outlines this proposed strategy for the selection of precipitate morphology in Mg alloys.

2. Material and methods

It is however difficult to validate the strategy as proposed in Fig. 1, using conventional experimental methods. This is because in bulk samples there are multiple obscuring factors that would make the result ambiguous, including the simultaneous activation of multiple deformation modes that interact (DT, basal and non-basal slips) [31], varying grain size and crystal orientations of different proportions, non-uniform spatial distribution of precipitates, as well as the frequent occurrence of detwinning. In order to pinpoint the obstructing effect of each type of precipitate morphology on $\{10\bar{1}2\}$ DT, we tested inside a transmission electron microscope (TEM) a series of Mg alloys, each being a microscale sample containing only a specific morphology. Since it is difficult to obtain all morphologies for a specific precipitate phase at one alloy composition, we used several alloys, including Mg-Al (AZ31), Mg-Zn (ZK60 and Z6), Mg-Y-Nd (WE54) and Mg-Gd-Y-Zn (GWZ931), to cover the whole range of shape of precipitates, such as particles, rods, plates and lamellar precipitates (Fig. 2). In order to exclude the effect of different solute species, precipitate phase/composition and lattice constant (e.g. c/a ratio), whenever possible we directly compared the twinning behavior and mechanical data from a same alloy system. To avoid the interference from basal slips, the compression loading axis for all the tested samples is aligned in parallel with the basal plane to ensure the dominancy of $\{10\bar{1}2\}$ DT.

3. Results and discussion

3.1. Microscopy observations

As shown in Fig. 2(a) and (b), and (Supplementary Materials) S4-S6, DT in pillars with dispersed particles, rods or nano plates behaved similarly to that in pure Mg pillars: a twin formed at the top of the pillar and finally engulfed almost the entire pillar. The densely distributed precipitates neither blocked twin growth, nor divided the twin into smaller pieces. The DT behavior was quite different when the precipitates were connected to each other. Fig. 2(c) shows a WE54 pillar where the precipitate formed a network: no twin could be detected. During compressive loading, the pillar underwent obvious plastic deformation, but the latter must be mediated by non-basal dislocation slip (see Fig. S3 for possible slip systems). This is in stark contrast to the test on another pillar containing two isolated plates fabricated from the same WE54 sample. In such a pillar, when applied stress reached a critical level, twin was nucleated and expanded towards the root part of the pillar (Fig. S7). Similar suppression of DT could also be achieved in GWZ931 pillars containing long-period-stacking-order (LPSO) lamellae (Fig. 2(d)). After this pillar was shortened along the axial direction by ~7%, only two small volumes were twinned. In contrast, in the test on another pillar containing less LPSO lamellae that was fabricated from the same GWZ931 sample, twinning still dominated the plastic deformation (Fig. S8). With the increasing volume fraction of

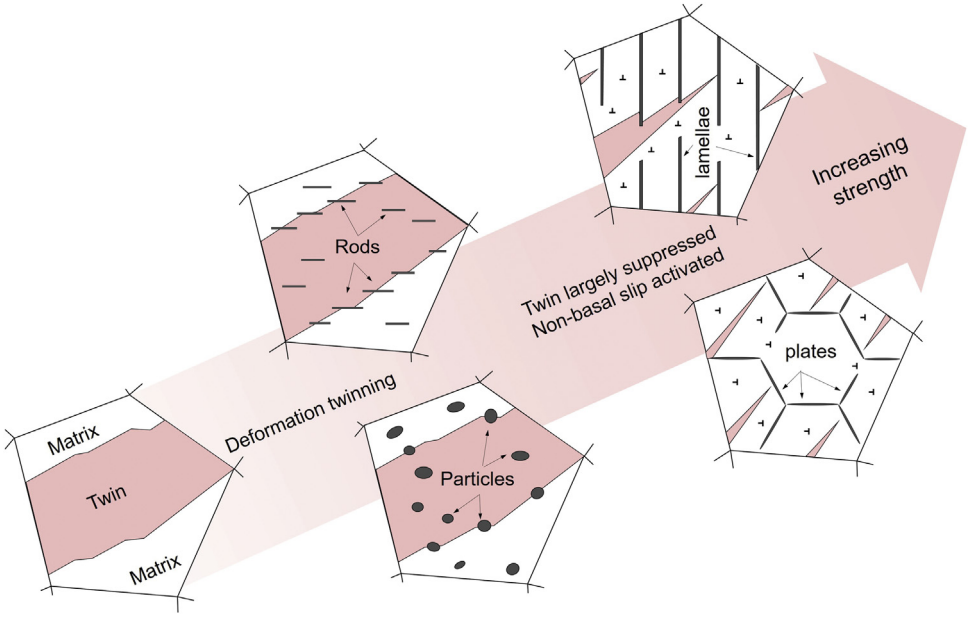

Fig 1. Criteria for precipitate morphology selection in the design of high-strength Mg alloys.

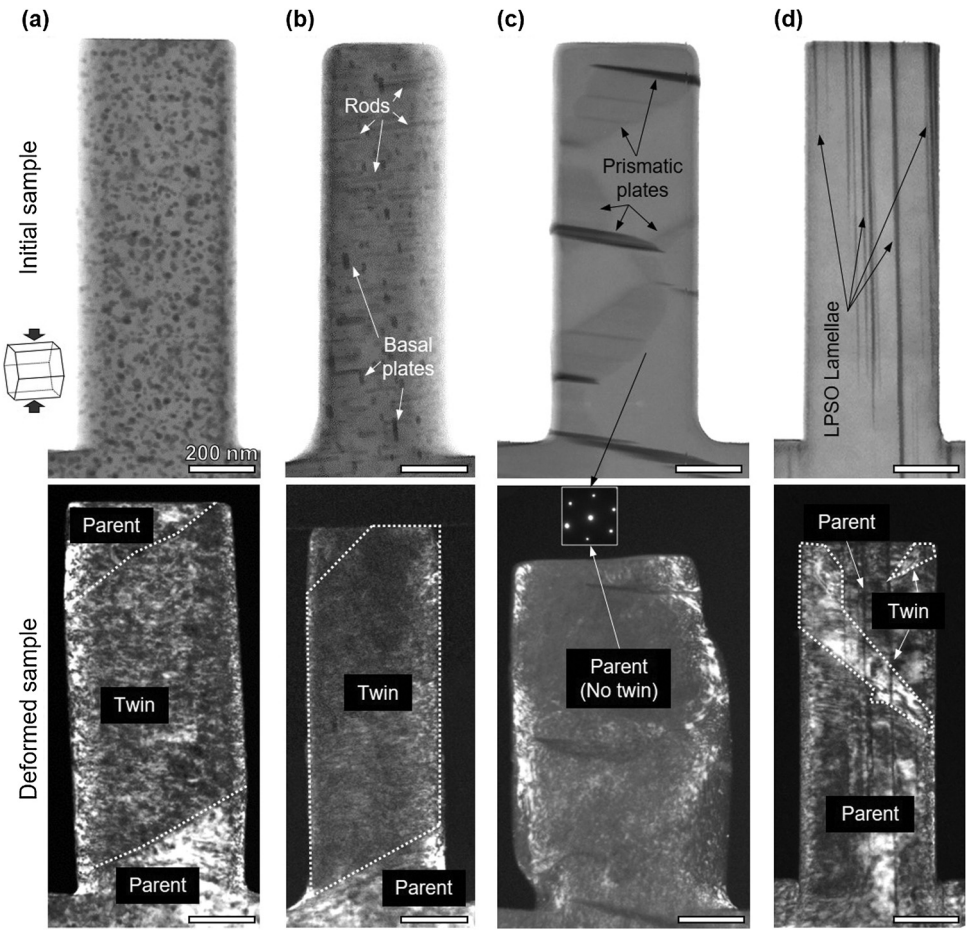

Fig. 2. In-situ TEM observation of the deformation behavior of Mg alloys with different precipitate morphology. Top row, bright field Scanning Transmission Electron Microscope (STEM) images showing initial samples. Bottom row, dark field TEM images showing deformed samples. In (a) ZK60 pillar with particles, (b) Z6 pillar with rods and a small number of nanoscale plates, almost the entire pillar is twinned. In (c) WE54 pillar with plate-network or in (d) GWZ931 pillar with LPSO lamellae, DT is significantly suppressed. Compressive loading was along the pillar axial orientation, which is parallel to the $\{0002\}$ plane (basal) of Mg. The observation (electron beam) direction is parallel to the basal plane in (a), (b), (d), and is parallel to the *c*-axis in (c). All scale bars, 200 nm.

LPSO lamellae, we found that twinning was generally reduced and finally eliminated (Fig. S9).

3.2. Mechanical responses

Next, we analyzed how precipitates influenced the measured stress-strain curves. Fig. 3(a) displays stress-strain curves of ZK60 pillar containing particles (red), Z6 pillar containing c-axis rods (blue), and pure Mg pillar (green). The curves of ZK60 and Z6 pillars exhibit a similar shape, and the flow stresses are at the same level. According to the *in situ* videos (Supplementary Video S1 and S2), in both pillars twinning set in when stress reached ~350 MPa. After that, twin thickened in a jerky way, as manifested in the stress-strain curve by several small strain bursts. From the *in situ* videos, these strain bursts and stress dropping appeared to correspond to a breaking away of the twin boundary from precipitates, reflecting the obstructing effect of precipitates on twin boundary migration. This is different from the smooth twin boundary migration in pure Mg pillars. During twin growth, the flow stress stayed at the level of ~400 MPa with no obvious work-hardening. Compared with pure Mg pillars, the yield and flow stresses of pillars containing particles or rods were improved by ~20%.

In WE54 pillars, the flow stresses were higher and the plastic flow was smoother (Fig. 3(b)). In the pillar with isolated prismatic plates (Supplementary Video S3 and Fig. S7(a)), the formation of DT was delayed to after 8% engineering strain. At this time, the corresponding stress approached ~500 MPa. In the pillar with plates that formed a network (Supplementary Video S4 and Fig. S7(b)), no twin formed and remarkable work-hardening could be observed after yielding. The peak stress was ~600 MPa (engineering strain ~10%). After that, the stress decreased, which might be related to the shearing of one plate.

High stresses could also be sustained in GWZ931 pillars (Fig. 3(c)). In the case with a few LPSO layers (Supplementary Video S5 and Fig. S8(a)), a twin formed then expanded under the stress of ~500 MPa. Very interestingly, increasing the number of LPSO layers (increasing volume fraction) was able to further suppress DT. This was accompanied by remarkable strengthening: the yield stress and flow stress reached ~620 MPa and ~700 MPa, respectively. From the *in situ* video (Supplementary Video S6 and Fig. S8(b)), only two small twins appeared. The first twin formed well beyond yielding, after ~4% engineering strain had already set in. This small twin terminated at one of the LPSO layers and did not grow further upon continued loading. Another small twin formed at ~5% strain, and grew with increasing applied strain.

3.3. Strain-component analysis

Both the visual *in situ* observations and the mechanical data indicate that the remarkable strengthening arises from the suppression of DT. To demonstrate that strengthening indeed originates from the switch in plasticity mechanism, we have carried out a "strain-

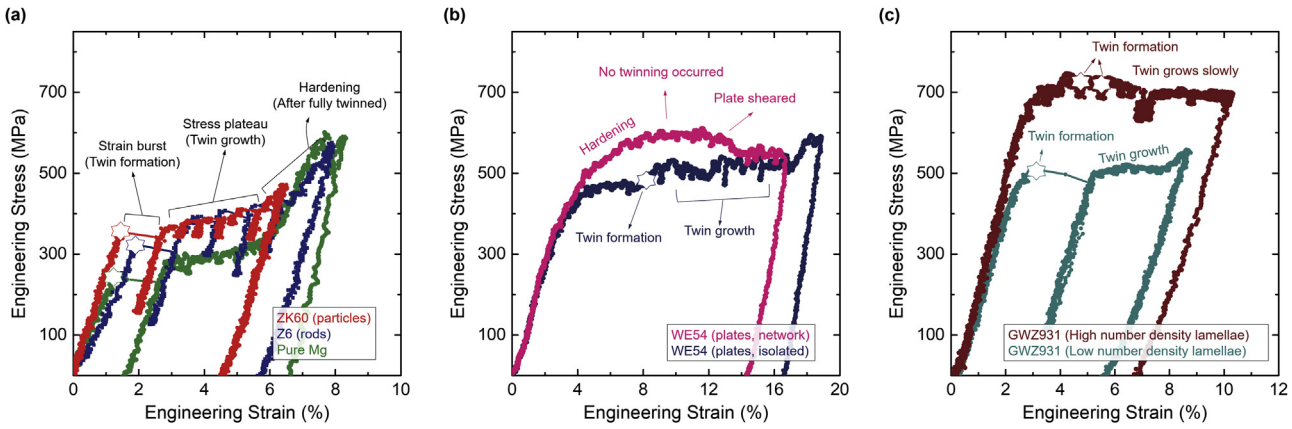

Fig. 3. Stress-strain curves of tested pillar with various precipitate morphology. (a) ZK60, Z6 and pure Mg pillar. (b) WE54 pillars. (c) GWZ931 pillars. The hexagram represents the twin formation.

component analysis" in Fig. 4, which displays the contribution of elastic strain ($\varepsilon_{elastic}$), dislocation-slip mediated strain ($\varepsilon_{dislocation}$) and twinning mediated strain (ε_{twin}) to the total engineering strain (ε_{total}) along the compression direction in the four pillars as shown in Fig. 2. All horizontal axes start from 1.5% to avoid the complex stress and strain condition when the indenter just contacts the pillar. The flow stress is seen to scale inversely with the contribution of twinning to the total plastic strain. For example, in pure Mg pillars (Supplementary Materials Fig. S10) and pillars with particles or rods (Fig. 4(a) and (b)), twinning starts at 1–2% strain and dom-

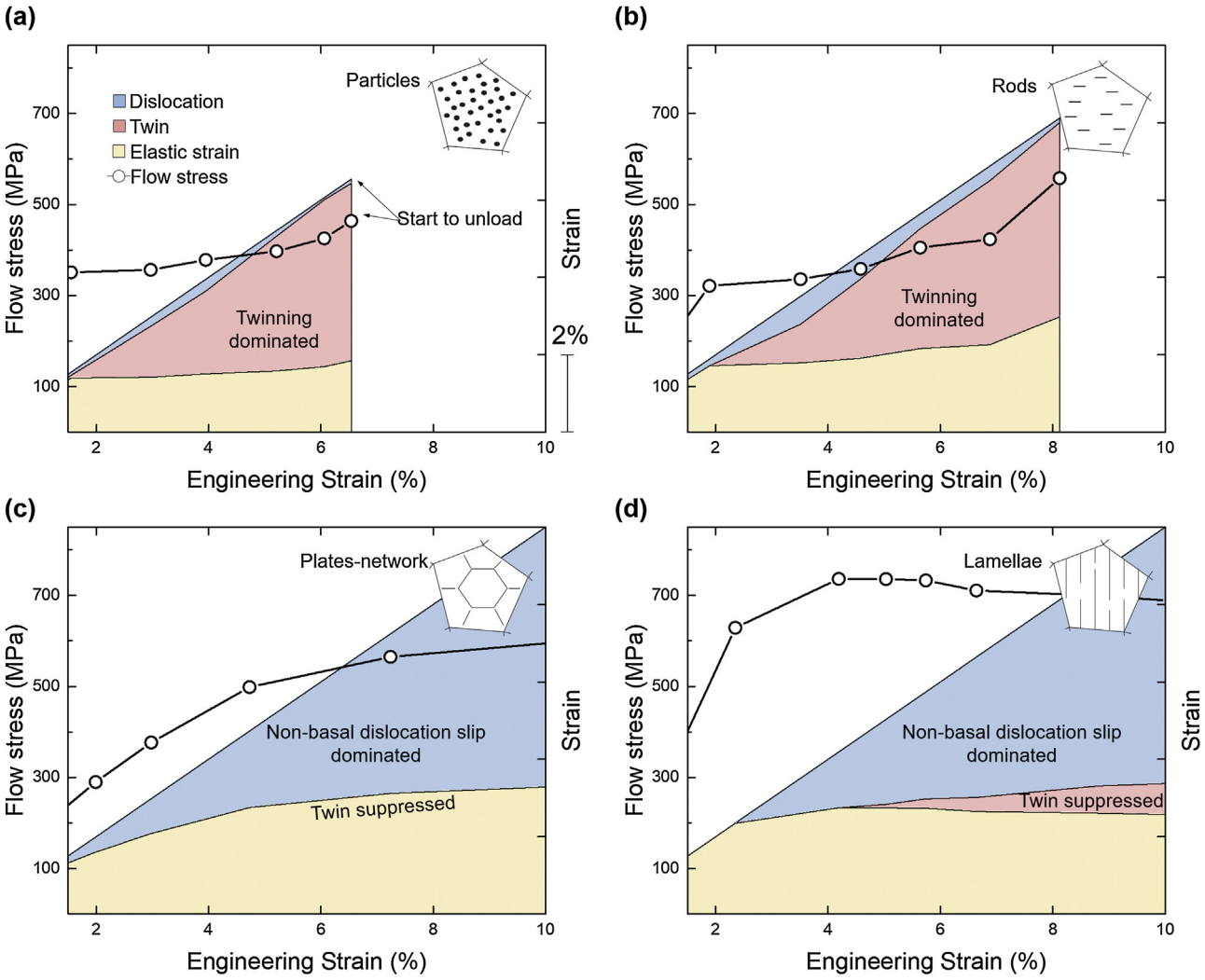

Fig. 4. Strain-component analyses demonstrating the trend that the suppression (promotion) of DT (dislocation slip) corresponds to higher strength. Diagrams showing the proportion of $\varepsilon_{elastic}$, $\varepsilon_{dislocation}$ and ε_{twin} in the ε_{total} along the programed straining process, overlapped with the flow stresses, in four tested pillars with particles (a), rods (b), plate-networks (c) and lamellae (d).

inates the plastic strain; this profuse twinning corresponds to a relatively low flow stress in a range of 250–400 MPa. It should be noted that the compressive loading direction was not always perfectly parallel to the basal plane. As a result, a small degree of basal slips is expected in the present experiments. In contrast, in the pillar with plate-network, DT was completely suppressed and dislocation slips dominated the plastic strain. The absence of twinning is tantamount to a much higher flow stress (Fig. 4(c)) and stronger strain hardening. Similarly, in the pillars with lamellar structures, only a small amount of twinning occurred after 4% strain and dislocation slip was the dominant plasticity carrier. The flow stress sustained went up to ~700 MPa (Fig. 4(d)).

3.4. Strengthening factors

The high strength obtained in our tested pillars can be attributed to the following factors: sample dimensions, solute atoms and precipitates. First, sample size effect. In accordance with the trend of "smaller is stronger [32]", the strength of micro-/nano-scale samples that have similar sizes for our pillars, was generally higher than that in bulk scale samples. However, the scale of $\sim 10^2$ nm was not small enough to eliminate the $\{10\bar{1}2\}$ DT. Twinning still dominated the plastic deformation in our pure Mg, Mg-Al and Mg-Zn pillars.

Second, solute atoms. In our experiments, because DT was still dominant in rare-earth (RE) free pillars, but suppressed in Mg-RE pillars (Mg-Y-Nd and Mg-Gd-Y-Zn), here we focused on Y, Nd and Gd. Such RE elements were found to have a strengthening effect for Mg alloys [33]. For Y, a high content of Y solutes was reported to reduce $\{10\bar{1}2\}$ DT [34]. The effect of Nd can be neglected here because they are expected to be completely consumed in forming precipitates [35]. For Gd, it has been reported that Gd dissolved in matrix couldn't obstruct the twin growth until they segregated on the twin boundary after annealing [36]. Therefore, in our WE54 and GWZ931 pillars, Y was expected to contribute to the suppression of DT. This could be one reason for the generally higher stress required for DT in Mg-RE pillars than in RE-free pillars. Nevertheless, in Mg-RE pillars, once nucleated, twin could still expand to large volume (Figs. S7(a) and S8(a)). Further suppression of DT required the optimization of precipitate morphology.

Third, precipitates. Since all WE54 pillars and GWZ931 pillars were fabricated from the same WE54 sample and GWZ931 sample, respectively, the solute species and concentration should be the same. Therefore, the change of DT behavior and strength should result from the change of precipitates only. In the WE54 pillar with two isolated prismatic plates, $\{10\bar{1}2\}$ DT could still nucleate and grow (Fig. S7(a)). The failure in suppressing $\{10\bar{1}2\}$ DT by prismatic plates was also reported in Ref. [10,14]. In contrast, in the WE54 pillar with plate-network, no $\{10\bar{1}2\}$ twin could be detected (Fig. S7(b)). Since such network structure (like a honeycomb) was only occasionally observed in local areas [37], the suppression of $\{10\bar{1}2\}$ DT was not observed in bulk WE54 alloys.

In GWZ931 pillars, the general trend is that high volume fraction of LPSO precipitates leads to less DT and higher flow stress. In the pillar shown in Fig. S9(d), there are three LPSO lamellae at left that are much thicker than the other two lamellae and all the lamellae in other pillars. In this pillar, twin was fully suppressed, and the highest strength was achieved (Fig. S9(e)). In contrast to the isolated particles, rods and plates, the LPSO lamellae have a high aspect ratio. First, this geometric configuration may provide large internal stress against the twin thickening [7,20]; Second, such wall-like barriers make it difficult for a twin to bypass or envelope, much like stopping flooding using a dam. Third, when the LPSO lamella encompasses the entire cross-section of the pillar, the Mg matrix is divided into nanoscale volumes (similar condition can also be reached by plate-networks). This imposes elastic and geometric constraints on DT. In metals with hexagonal close packed structure (e.g. Mg), DT is known to be much more grain size aware than the dislocation slip [38]. In small volumes the nucleation stress for DT would dramatically increase, giving way to dislocation slip as the dominant plastic carrier. One can expect that DT will be effectively suppressed when the spacing between each LPSO lamella is smaller enough (akin to grain refinement). Moreover, the probability of a twin being arrested will increase when the LPSO lamella possesses larger area. Therefore, LPSO lamellae with fine spacing and large area (encompasses the entire grain) could be the effective strengthening structure to reduce DT and enhance the strength of Mg alloys.

4. Conclusion

Our systematic dataset verified the proposal in Fig. 1, which inspires future designs of high strength Mg alloys. One desirable microstructure that comes to mind is the honeycomb arrangement of prismatic plates, which has been occasionally observed in local areas in Mg-Sm alloys [39] or in Mg-Y-Nd alloys [40]. Note that prismatic plates also have a strong obstructing effect on basal slips [8,10]. The next step is to understand the general conditions needed for the widespread formation of such three-dimensional network microstructure in Mg alloys. Finally, we note that the *in situ* testing-imaging methodology in the present work enables a fast screening of potential strengthening microstructures, and as such represents a step-forward in implementing the strategy prescribed in the "Materials Genome Initiative" for accelerating the design of high-performance alloys.

Acknowledgements

Z.W.S. and B.Y.L. acknowledge the supports by the National Key Research and Development Program of China (Nos. 2017YFB0702001), National Natural Science Foundation of China (Nos. 51601141, 51231005 and 51621063), and the Science and Technology Department of Shaanxi Province (Nos. 2016KTZDGY-04-03 and 2016KTZDGY-04-04). B.Y.L. thanks the support from the China Postdoctoral Science Foundation (2016M600788).

Appendix A. Supplementary data

Supplementary data associated with this article can be found, in the online version, at https://doi.org/10.1016/j.jmst.2018.01.017.

References

[1] X.J. Wang, D.K. Xu, R.Z. Wu, X.B. Chen, Q.M. Peng, L. Jin, Y.C. Xin, Z.Q. Zhang, Y. Liu, X.H. Chen, G. Chen, K.K. Deng, H.Y. Wang, J. Mater, Sci. Technol. (2017), http://dx.doi.org/10.1016/j.jmst.2017.07.019.
[2] W.J. Joost, P.E. Krajewski, Scr. Mater. 128 (2017) 107–112.
[3] S.P. Ringer, K. Hono, Mater. Charact. 44 (2000) 101–131.
[4] J.F. Nie, Metall. Mater. Trans. A 43 (2012) 3891–3939.
[5] E.W. Kelley, W.F. Hosford, Trans. Metall. Soc. AIME 242 (1968) 5–13.
[6] J.F. Nie, Scr. Mater. 48 (2003) 1009–1015.
[7] J.D. Robson, N. Stanford, M.R. Barnett, Acta Mater. 59 (2011) 1945–1956.
[8] P. Hidalgo-Manrique, J.D. Robson, M.T. Pérez-Prado, Acta Mater. 124 (2017) 456–467.
[9] N. Stanford, M.R. Barnett, Mater. Sci. Eng. A 516 (2009) 226–234.
[10] S.R. Agnew, R.P. Mulay, F.J. Polesak, C.A. Calhoun, J.J. Bhattacharyya, B. Clausen, Acta Mater. 61 (2013) 3769–3780.
[11] J.T. Wang, N. Stanford, Acta Mater. 100 (2015) 53–63.
[12] J. Jain, P. Cizek, W.J. Poole, M.R. Barnett, Mater. Sci. Eng. A 647 (2015) 66–73.
[13] S.R. Kada, P.A. Lynch, J.A. Kimpton, M.R. Barnett, Acta Mater. 119 (2016) 145–156.
[14] M. Lentz, M. Klaus, M. Wagner, C. Fahrenson, I.J. Beyerlein, M. Zecevic, W. Reimers, M. Knezevic, Mater. Sci. Eng. A 628 (2015) 396–409.
[15] N. Stanford, J. Geng, Y.B. Chun, C.H.J. Davies, J.F. Nie, M.R. Barnett, Acta Mater. 60 (2012) 218–228.
[16] J.B. Clark, Acta Metall. 16 (1968) 141–152.

[17] M.A. Gharghouri, G.C. Weatherly, J.D. Embury, Philos. Mag. A 78 (1998) 1137–1149.
[18] J. Robson, N. Stanford, M. Barnett, Metall. Mater. Trans. A 44 (2013) 2984–2995.
[19] M. Matsuda, S. Ii, Y. Kawamura, Y. Ikuhara, M. Nishida, Mater. Sci. Eng. A 386 (2004) 447–452.
[20] J.D. Robson, Acta Mater. 121 (2016) 277–287.
[21] M.R. Barnett, Mater. Sci. Eng. A 464 (2007) 1–7.
[22] B.Y. Liu, J. Wang, B. Li, L. Lu, X.Y. Zhang, Z.W. Shan, J. Li, C.L. Jia, J. Sun, E. Ma, Nat. Commun. 5 (2014) 3297.
[23] B.-Y. Liu, L. Wan, J. Wang, E. Ma, Z.-W. Shan, Scr. Mater. 100 (2015) 86–89.
[24] Q. Zu, X.-Z. Tang, S. Xu, Y.-F. Guo, Acta Mater. 130 (2017) 310–318.
[25] C.D. Barrett, H. El Kadiri, Acta Mater. 63 (2014) 1–15.
[26] P.G. Partridge, E. Roberts, Acta Metall. 12 (1964) 1205–1210.
[27] X.Y. Zhang, B. Li, X.L. Wu, Y.T. Zhu, Q. Ma, Q. Liu, P.T. Wang, M.F. Horstemeyer, Scr. Mater. 67 (2012) 862–865.
[28] J. Wang, L. Liu, C.N. Tomé, S.X. Mao, S.K. Gong, Mater. Res. Lett. 1 (2013) 81–88.
[29] J. Geng, Y.B. Chun, N. Stanford, C.H.J. Davies, J.F. Nie, M.R. Barnett, Mater. Sci. Eng. A 528 (2011) 3659–3665.
[30] X.H. Shao, S.J. Zheng, D. Chen, Q.Q. Jin, Z.Z. Peng, X.L. Ma, Sci. Rep. 6 (2016) 30096.
[31] J. Xu, B. Guan, H. Yu, X. Cao, Y. Xin, Q. Liu, J. Mater. Sci. Technol. 32 (2016) 1239–1244.
[32] M.D. Uchic, D.M. Dimiduk, J.N. Florando, W.D. Nix, Science 305 (2004) 986–989.
[33] G. Li, J. Zhang, R. Wu, Y. Feng, S. Liu, X. Wang, Y. Jiao, Q. Yang, J. Meng, J. Mater, Sci. Technol. (2017), http://dx.doi.org/10.1016/j.jmst.2017.12.011, in press.
[34] N. Stanford, R.K.W. Marceau, M.R. Barnett, Acta Mater. 82 (2015) 447–456.
[35] J.J. Bhattacharyya, F. Wang, P.D. Wu, W.R. Whittington, H.E. Kadiri, S.R. Agnew, Int. J. Plast. 81 (2016) 123–151.
[36] J.F. Nie, Y.M. Zhu, J.Z. Liu, X.Y. Fang, Science 340 (2013) 957–960.
[37] Z. Xu, M. Weyland, J.F. Nie, Acta Mater. 75 (2014) 122–133.
[38] Q. Yu, Z.-W. Shan, J. Li, X. Huang, L. Xiao, J. Sun, E. Ma, Nature 463 (2010) 335–338.
[39] M. Nishijima, K. Hiraga, M. Yamasaki, Y. Kawamura, Mater. Trans. 50 (2009) 1747–1752.
[40] H. Liu, Y. Gao, Z. Xu, Y.M. Zhu, Y. Wang, J.F. Nie, Sci. Rep. 5 (2015) 16530.